Inter-Network High-Order Functional Connectivity (IN-HOFC) and its Alteration in Patients with Mild Cognitive Impairment

Han Zhang, Panteleimon Giannakopoulos, Sven Haller, Dinggang Shen, Seong-Whan Lee & Shijun Qiu

Neuroinformatics

ISSN 1539-2791

Neuroinform
DOI 10.1007/s12021-018-9413-x

Springer

Neuroinformatics
https://doi.org/10.1007/s12021-018-9413-x

ORIGINAL ARTICLE

Inter-Network High-Order Functional Connectivity (IN-HOFC) and its Alteration in Patients with Mild Cognitive Impairment

Han Zhang [1] · Panteleimon Giannakopoulos [2] · Sven Haller [3,4,5,6] · Dinggang Shen [1,7] · Seong-Whan Lee [7] · Shijun Qiu [8]

Abstract

Little is known about the high-order interactions among brain regions measured by the similarity of higher-order features (other than the raw blood-oxygen-level-dependent signals) which can characterize higher-level brain functional connectivity (FC). Previously, we proposed FC topographical profile-based high-order FC (HOFC) and found that this metric could provide supplementary information to traditional FC for early Alzheimer's disease (AD) detection. However, whether such findings apply to network-level brain functional integration is unknown. In this paper, we propose an extended HOFC method, termed inter-network high-order FC (IN-HOFC), as a useful complement to the traditional inter-network FC methods, for characterizing more complex organizations among the large-scale brain networks. In the IN-HOFC, *both* network definition *and* inter-network FC are defined in a high-order manner. To test whether IN-HOFC is more sensitive to cognition decline due to brain diseases than traditional inter-network FC, 77 mild cognitive impairments (MCIs) and 89 controls are compared among the conventional methods and our IN-HOFC. The result shows that IN-HOFCs among three temporal lobe-related high-order networks are dampened in MCIs. The impairment of IN-HOFC is especially found between the *anterior* and *posterior* medial temporal lobe and could be a potential MCI biomarker at the network level. The competing network-level low-order FC methods, however, *either* revealing less *or* failing to detect any group difference. This work demonstrates the biological meaning and potential diagnostic value of the IN-HOFC in clinical neuroscience studies.

Keywords Functional magnetic resonance imaging (fMRI) · Mild cognitive impairment (MCI) · Alzheimer's disease (AD) · Functional connectivity · Brain network · High-order

Introduction

The brain functional network has long been an attractive research topic with help from functional magnetic resonance imaging (fMRI) (Menon 2011; Varoquaux and Craddock 2013; Zhang and Raichle 2010). The analysis of various functional networks has become one of the powerful tool facilitating our understanding of large-scale brain functional organization (Bullmore and Sporns 2009; Smith et al. 2013; Stam et al. 2015). One of the most important network characteristics is the highly-modularized and hierarchical functional architecture, defined by the multi-way directed and undirected

✉ Dinggang Shen
dgshen@med.unc.edu

✉ Shijun Qiu
qiu-sj@163.com

Seong-Whan Lee
sw.lee@korea.ac.kr

[1] Department of Radiology and BRIC, University of North Carolina at Chapel Hill, CB#7513, 130 Mason Farm Road, Chapel Hill, NC 27599, USA

[2] Division of Psychiatry, Geneva University Hospitals, Geneva, Switzerland

[3] Affidea CDRC - Centre Diagnostique Radiologique de Carouge, Carouge, Switzerland

[4] Department of Surgical Sciences, Radiology, Uppsala University, Uppsala, Sweden

[5] Department of Neuroradiology, University Hospital Freiburg, Freiburg, Germany

[6] Faculty of Medicine, University of Geneva, Geneva, Switzerland

[7] Department of Brain and Cognitive Engineering, Korea University, Seoul 02841, Republic of Korea

[8] Department of Radiology, The First Affiliated Hospital of Guangzhou University of Chinese Medicine, 16 Jichang Road, Guangzhou 510405, Guangdong, China

Published online: 09 February 2019

functional connectivity (FC) among functional networks (Allen et al. 2011; Bellec et al. 2010; Cordes et al. 2002; Kiviniemi et al. 2009; Lee et al. 2012; Mezer et al. 2009; Newman 2006; Qiao et al. 2016; Sporns and Betzel 2015; Stevens et al. 2009). This characteristic is believed to facilitate information exchanges between remote brain regions (Misic et al. 2015). With such merit, brain network modeling and inter-network connectivity have long been used to detect neuroimaging biomarkers of brain diseases (Barkhof et al. 2014; Greicius 2008; Jafri et al. 2008; Liang et al. 2015; Zhang et al. 2016a; Zhang et al. 2017b; Zhu et al. 2014).

Various modeling methods have been proposed to reveal the multi-facet characteristics of the inter-network connectivity. Some of them utilized a simple metric to assess the interaction among networks, i.e., Pearson's correlation between blood-oxygen-level-dependent (BOLD) time series of any pair of networks (Jafri et al. 2008; Yang et al. 2016) and directed interaction between the networks (Karunanayaka et al. 2014). These methods first construct networks based on inter-regional synchronization of the BOLD time series, and then using the network's activity (e.g., the averaged BOLD signal within each network) as an input to calculate inter-network FC (Brier et al. 2012; Jafri et al. 2008; Yang et al. 2016). The similarity of all these methods is that they directly use BOLD time series to calculate the inter-network connectivity. That is, BOLD signals are the features used in *both* network construction *and* inter-network FC calculation (Bijsterbosch et al. 2014; Jafri et al. 2008; Putcha et al. 2015; Wang et al. 2014). In other words, brain networks can be derived from clustering, modular analysis, or independent component analysis (ICA); and then network-level BOLD time courses were extracted and correlated between each pair of them, resulting in inter-network FC. Since BOLD signals are the measurements reflecting brain activity, inter-network FC calculated from BOLD signals (low-order features) may only reflect simple (low-order) inter-network interactions. That is, these methods cannot model more complex, higher-level relationship among the brain networks. Note that here we use the prefix "low-order" that is similar to the low-level or low-order features widely used in the machine learning field, which describes a feature measuring relatively simple aspects of an object, such as pixel intensity to a natural image. The "high-order" features, on the other hand, measure more complex attributes, such as context and distribution of the image. Thus, it is necessary to investigate networks' high-order FC for neuroscience studies.

Previous studies have shown that the topographic FC profile of a brain region is informative (Wang et al. 2016; Zhang et al. 2016b), and that the similarity analysis based on these "high-order" profiles is also feasible to calculate inter-regional functional associations (Cohen et al. 2008; Hirose et al. 2013; Nelson et al. 2010; Wang et al. 2016). In our previous observations (Jia et al. 2017; Zhang et al. 2016a; Zhang et al. 2017a, b, c, Zhao et al. 2018), we found that two brain regions may have quite similar FC topographic profiles with respect to other regions, even though they belong to traditionally-believed different functional networks (i.e., they have low FC due to less correlated BOLD signals). We thus proposed *high-order FC* (HOFC) computed based on further correlation of regional topographic FC profiles (describing how a region connects with other regions), which could provide essential complementary information to the traditional FC using raw BOLD time series in brain disease studies (Jia et al. 2017; Zhang et al. 2016a, b). HOFC is believed to be able to reflect a high-level and indirect relationship between two brain regions, as both of them could be similarly connected to the same group of other regions. However, traditional FC only measures a direct connection with temporally synchronized BOLD signals. Therefore, regions with high HOFC do not necessarily indicate a high traditional FC between two brain regions but rather suggest that the two regions behave similarly (have similar FC topographical profiles) in the context of global connectome at a systemic level. We have demonstrated that the HOFC between the anterior and the posterior cingulate cortex was 0.71 whereas their FC was only 0.24 (Zhang et al. 2016a). This indicates that, although their BOLD signals are less similar to each other, they both mediate high-level cognitive functions by connecting with similar other regions; thus, from a high-level function point of view, they could be functionally more similar. We also found that the HOFC could provide essential supplementary information to the conventional FC-based brain disease study, with increased sensitivity in disease detection, including early Alzheimer's disease (AD) detection (Jia et al. 2017; Zhang et al. 2016a, b, c; Zhao et al. 2018). More importantly, this HOFC seems to be test-retest reliable (Zhang et al. 2017a).

In this paper, we propose that HOFC can be calculated not only between different brain regions but also between different brain functional networks. Such a network-level HOFC can be used for better investigations of cognitive impairments in a *large scale* at the *systemic level* (Karunanayaka et al. 2014; Kong et al. 2014; Menon 2011; Wang et al. 2014). The investigation of network-level HOFC could reveal novel biomarkers which might sit at the high level in the brain functional hierarchy (while region-wise HOFC analysis mainly focusing on the low-level brain functional hierarchy). Therefore, network-level HOFC could provide another view angle and complementary information compared to traditional network-level FC studies (Jafri et al. 2008) for a better understanding of brain diseases. Specifically, pairwise regional HOFC can be extended to measure high-order functional relationship for all the region pairs, from which several large-scale brain networks can be identified based on the FC topographical similarity among multiple brain regions. Of note, such large-scale brain functional networks are defined in a high-order manner, rather than based on the similarity of the regional BOLD signals (i.e., in a low-order manner). Such a high-order network formation can be easily achieved by

grouping brain regions, enhancing the similarity of FC topographic profiles within the same functional system and the dissimilarity of them between distinct functional systems at the same time (Wig et al. 2014). Then, by calculating a second round of the correlations between each pair of the network-specific FC topographical profiles, one can generate "inter-network high-order functional connectivity (IN-HOFC)".

In the following sections of this paper, we briefly described the HOFC method for better introducing the IN-HOFC in Section 2.1. We then applied the IN-HOFC method to detect group differences between mild cognitive impairment (MCI) patients and normal controls for detection of early AD biomarkers in the following sections. We hypothesized that the IN-HOFC can detect not only the biomarkers found based on traditional network FC studies, such as the default mode network (DMN) (Bai et al. 2008; Li et al. 2015; Nickl-Jockschat et al. 2012), but also additional abnormalities in other functional networks.

Materials and Methods

IN-HOFC: Calculating High-Order FC between Networks

General Descriptions of HOFC and IN-HOFC

By using a clustering strategy (Bellec et al. 2010; Yeo et al. 2011), we can construct "high-order functional networks" based on pairwise HOFC among all brain regions. In this way, different brain regions with similar topographical FC profiles (rather than similar regional BOLD signals) can be grouped into the same high-order network (thus, such a network could be different from the traditional FC-based network). The main motivation to form the high-order functional networks comes from our observation that many brain regions share similar FC topographic profiles and there is structured information inside of the FC profiles of all regions (Zhang et al. 2016a, a). After grouping them into subgroups, we can extract network-wise FC profiles and, the second round of Pearson's correlation based on these network-specific FC profiles can be conducted to generate HOFC among these networks. In traditional functional network connectivity studies (Jafri et al. 2008), it is the low-level, BOLD fluctuations that are used for inter-network FC calculation. In contrast, in IN-HOFC, the high-level, FC topographic profiles were correlated. Moreover, the network detection in IN-HOFC is based on high-order features, rather than the BOLD signals. It is important to note that, since HOFC was found to be different from FC (Jia et al. 2017; Zhang et al. 2016a), IN-HOFC can also be different from the traditional functional network connectivity.

Specifically, IN-HOFC consists of four major stages: **1)** Individual-level FC topographic profiles generation, based on Pearson's correlation of regional mean BOLD time series; **2)** Group-level high-order network generation, integrating a *k*-means clustering based on subject-concatenated FC profiles to detect common high-order functional networks across all subjects while maintaining network correspondence across different subjects; **3)** Individual-level high-order network interaction analysis, consisting of individual network-wise FC profile extraction based on the group-level high-order network partition, as well as the second round of correlation analyses on these network-wise FC profiles; and **4)** Statistical analysis of the individual IN-HOFC to detect group differences. The flowchart of the proposed method is shown in Fig. 1, with the details provided below.

FC Matrix Generation (Stage I)

According to a predefined brain atlas, each subject's brain can be partitioned into M regions. The length-T regional mean BOLD time series of every brain region can be extracted from the preprocessed fMRI data (Fig. 1a). Then, the Pearson's correlation between the BOLD time series (Fig. 1b) from any pair of brain regions can be computed and used to generate an $M \times M$ individual-level FC matrix for each subject (Fig. 1c). This FC matrix was further transformed into z-scores using the Fisher's r-to-z transformation. The individual-level FC matrices will be used as features in HOFC calculation as described below.

Group-level Feature-based Network Generation (Stage II)

After the pairwise HOFC matrices are calculated in Stage I, they will be used for clustering analysis to generate group-level high-order functional networks. Mathematically, the clustering results are actually the specific partitions of the FC feature matrix $\mathbf{F}^i$ for the i-th subject; and the parcellation way $\mathbf{P}^i$ on the $\mathbf{F}^i$, i.e., $\mathbf{F}^i \rightarrow^{\mathbf{P}^i} \left\{\mathbf{F}_1^i, \mathbf{F}_2^i, \cdots, \mathbf{F}_K^i\right\}$, depends on the inherent relationship among all columns of $\mathbf{F}^i$. In this way, network generation is inherently high order. Theoretically, for each subject, clustering can be conducted separately, i.e., grouping M FC feature vectors of M brain regions into K subgroups according to the similarity of the M vectors in a $\mathbf{R}^{M \times M}$ feature space. However, individual-level clustering does not guarantee correspondence of the clustering results across different subjects. Therefore, we adopted a group-level clustering strategy based on subject-concatenated FC profiles by stacking multiple $\mathbf{F}^i$ from all N subjects, i.e., $\mathbf{F} = [\mathbf{F}^1, \mathbf{F}^2, \cdots, \mathbf{F}^N]^{\mathrm{T}}$ (Fig. 1d) to keep the grouping consistent across subjects. Based on the similarity metric defined by Pearson's correlation between any pair of M columns from $\mathbf{F}$ (Fig. 1e), k-means clustering is applied, identifying K clusters in the $\mathbb{S}^{(M \times N) \times (M \times N)}$ feature space (Fig. 1f).

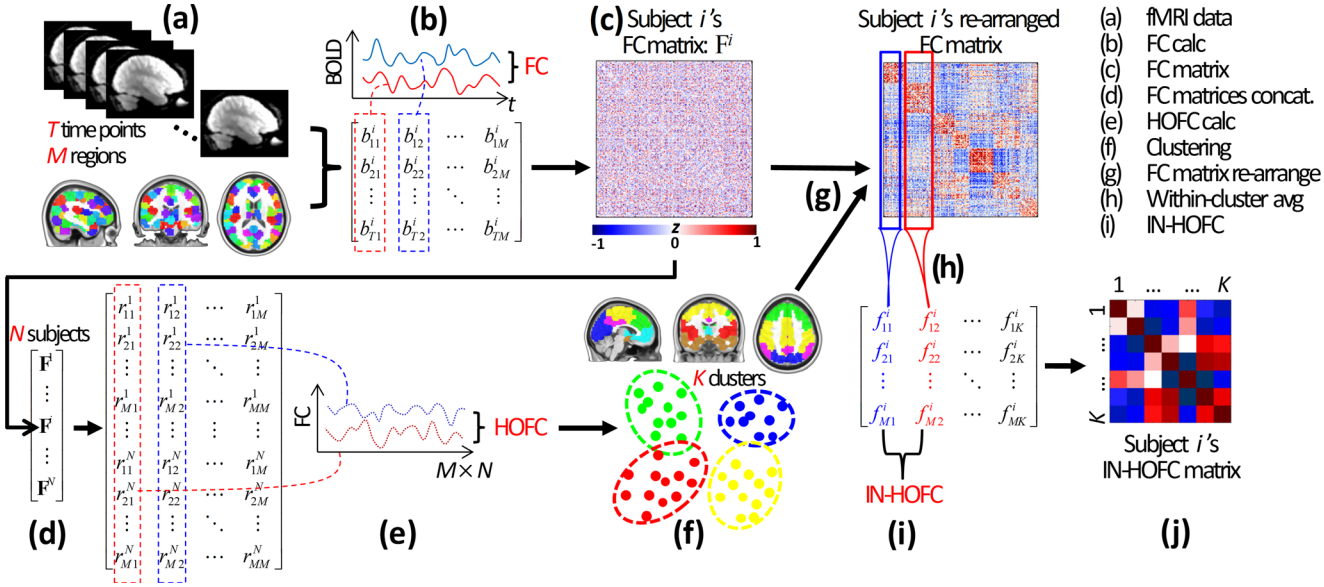

Fig. 1 Flowchart of IN-HOFC analysis. The algorithm consists of nine major steps (**a**–**i**), which are also summarized in the upper right. Individual FC matrix (**c**) is calculated for each subject based on the preprocessed fMRI data (**a**) and a predefined brain atlas consisting of *M* brain regions. Each element of the FC matrix represents Pearson's correlation coefficient r (which is further transformed to z score) between region-averaged BOLD time courses of two brain regions (**b**). All individual FC matrices from *N* subjects are concatenated to form a big matrix with the size of $(M \times N) \times M$ (**d**). The Pearson's correlation on each pair of the columns in this big matrix is a measure of HOFC (**e**), based on which k-means clustering is applied, grouping *M* brain regions into *K* clusters (or HOFC networks) at the group level (**f**). Based on the group-level partitions, each individual FC matrix is re-arranged (**g**). This is done by putting the regions within the same HOFC networks next with each other (re-ordering the columns and rows of the FC matrix). Then, network-specific FC features are extracted by averaging all columns within the same network/cluster (**h**). Finally, Pearson's correlation between each pair of network-specific FC features produces IN-HOFC (**i**) and finally, generates IN-HOFC matrix (**j**)

Individual-Level IN-HOFC Generation (Stage III)

Each subject's individual-level high-order functional networks can be generated by applying the clustering result generated at the group-level to individual FC feature matrix $\mathbf{F}^i$. Specifically, for each subject, the FC profiles (i.e., the column vectors in Fig. 1c) belonging to the same group-level cluster are first regrouped together (by rearranging) using region-to-network belongingness information derived from the latter step (Fig. 1g) and then averaged (Fig. 1h) to generate network-wise FC profiles (Fig. 1i) (Bijsterbosch et al. 2014). Next, Pearson's correlations of all pairs of network-wise FC profiles were computed to produce the individual-level IN-HOFC matrix (Fig. 1j), where each element represented the high-order linear interaction between two large-scale networks.

Group Inference (Stage IV)

Based on all the individual IN-HOFC matrices, a statistical comparison can be conducted to make a group-level inference (e.g., detection of group difference between patients and controls). In the Sections 2.2–2.6, we apply the proposed method to a real fMRI dataset from MCI subjects and normal aged elderly subjects to demonstrate the feasibility of our method in the detection of potential network-level biomarkers of the AD. We also compare the results from our method and other low-order inter-network FC methods in Section 2.7.

Participants

The real fMRI data we used consists of eighty MCI patients and 90 healthy normal-aging controls (CON). All of them were right-handed. None reported a history of neurological or psychiatric disorders. This study was approved by the local ethical committee. Informed written consent was obtained from all participants prior to inclusion in this study. One subject from CON was excluded due to excessive head motion (translation >1.5 mm or rotation >1.5°), and three MCI patients were excluded because of bad registration. Therefore, data from 89 CONs (29 males, 60 females, age 72.93 ± 4.24 years) and 77 MCIs (25 males, 52 females, age 72.82 ± 5.67 years), totally 166 subjects, were used. A full description of the subjects is listed in Table 1. Previous studies have shown that AD, which many MCI patients will convert to in following years, is a large-scale disconnectivity syndrome (Supekar et al. 2008), and that MCI has quite similar early connectivity alterations to that of the AD (Yao et al. 2010). Therefore, we planned to validate our method by examining the IN-HOFC differences between MCI and CON groups.

Table 1 Demographic, clinical and behavioral information

Variables	MCI	CON	*p* value
Total number of subjects	77	89	
Gender (male/female)	25/52	29/60	0.99
Age (yrs)			
Range	58–87	60–87	
Mean ± SD	72.82 ± 5.67	72.93 ± 4.24	0.52
Education (P/H/U[1])	6/37/34	18/41/30	0.06
MMSE			
Range	23–30	24–30	
Mean ± SD	27.53 ± 1.59	28.4 ± 1.29	0.0005*
CDR[2]	0.5	0	–
IADL	13.22 ± 8.72	8.16 ± 0.66	<0.0001*
Trail making test (B/A)	2.89 ± 1.19	2.74 ± 1.22	0.32
Phonemic verbal fluency	18.4 ± 6.54	21.4 ± 5.58	0.002*
RI-48 cued recall			
Immediate verbal cued recall	35.14 ± 5.09	38.84 ± 5.3	<0.0001*
Total free recall	15.69 ± 4.19	26.85 ± 5.4	<0.0001*
Instrusions	4.33 ± 5.66	1.70 ± 1.68	<0.0001*
Backward digit span[3]	3.20 ± 2.88	3.94 ± 3.18	0.13
Backward visuomemory span[3]	2.48 ± 3.25	4.82 ± 3.54	<0.0001*

[1]Primary (< 9 yrs)/High school (9–12 yrs)/University (> 12 yrs); [2]All CONs had the same CDR scores of 0, and all MCIs had the same CDR scores of 0.5; [3]Several MCIs and/or CONs did not complete the test due to impairment, whose scores were set to 0

*Significant group difference ($p < 0.05$). *MCI* mild cognitive impairment, *CON* normal control, *MMSE* mini mental state examination, *CDR* clinical dementia rating scale, *IADL* Lawton's instrumental activities of daily living scale

Experiments

A battery of neuropsychological and cognitive tests was conducted, including education level, Mini-Mental State Examination (MMSE), the Lawton's Instrumental Activities of Daily Living Scale (IADL), Clinical Dementia Rating scale (CDR), trail making, backward digit span, backward visual memory span, and RI-48 cued recall test and phonemic verbal fluency test. MCI and CON classifications were based on Petersen's criteria according to all the testing scores adjusted for age and education (Petersen et al. 2001). For more details, please see our previous studies (Zhang et al. 2016a). A simple block-designed CO_2 challenge task was conducted during fMRI acquisition. This task was designed for better identification of MCI according to their abnormal cerebrovascular reactivity triggered by hypercapnia (Richiardi et al. 2015) and was used after removing the task-induced responses to mimic "resting-state" fMRI data in the previous FC studies (Zhang et al. 2016a). Briefly, the experiment consists of 1 min normal breathing through the nose with air (OFF), 2 min normal breathing through the nose with 7% CO_2 with synthetic air (ON), 2 min OFF, 2 min ON, and 2 min OFF. Of note, the task effect was minimized by asking subject breathe normally through the nose via a nasal cannula instead of a tight facemask. No visual or auditory cue was presented. We think that the attention, alertness, even the autonomic processing could not be so different from that in the resting state.

Data Acquisition and Preprocessing

The fMRI data acquisition was performed on a whole-body 3.0 T MR scanner (TRIO, Siemens medical systems, Erlangen, Germany) using a standard echo-planar imaging sequence with an acquisition matrix = 74 × 74, 45 slices, slice thickness = 3 mm, voxel size = 2.97 × 2.97 × 3 mm^3, echo time (TE)/repetition time (TR) = 30/3000 ms, and 180 repetitions (9 min). T1-weighted structure MRI data were also collected for registration purpose but not analyzed in this study that mainly focused on functional connectivity.

The fMRI data preprocessing were conducted using Matlab version 2013a (the MathWorks, Inc., Natick, MA) and SPM8 (www.fil.ion.ucl.ac.uk/spm), including slice-timing, motion correction, registration to the standard space based on T1 New Segment in SPM8, spatial smoothing using a 6-mm full-width-half-maximum isotropic Gaussian kernel, de-trending, band-pass filtering (0.01–0.08 Hz), and nuisance regressing (removing task effect, mean signals in the cerebrospinal fluid and white matter masks, as well as the head motion parameters). The task effect was modeled using the task-related square wave convoluted with a canonical hemodynamic response function in SPM8. A post hoc visual inspection revealed that the significant task-induced fluctuations in BOLD signals were removed, leaving the data suitable for FC analysis (Zhang et al. 2016a).

IN-HOFC Calculation

FC Topographic Profiles

The atlas generated by Craddock et al. (2012) was used to parcellate the brain into 200 regions. Mean BOLD time series of each of the 200 brain regions were extracted from the preprocessed fMRI data of each subject. Of note, individual grey matter masks were not applied to the atlas during BOLD time series extraction, thus potential grey matter atrophy could affect the result. The feature matrix $\mathbf{F}^i$ was then generated and further concatenated across subjects, for forming a prolonged feature matrix $\mathbf{F}$ with the size of 33,200 × 200 (33,200 = 200 regions × 166 subjects) for our case of totally 166 subjects.

Group-Level Clustering

According to the recommendation of data-driven group-level analysis (Calhoun et al. 2001; Filippini et al. 2009), we used all data to conduct group-level clustering to ensure the feasibility of group comparisons. *K*-means clustering was applied to $\mathbf{F}$ to

cluster 200 prolonged feature vectors into 8 clusters or high-order networks. In other words, all the 200 brain regions were grouped into multiple subsets, each containing several regions with similar FC topographic profiles across subjects. The number of clusters was determined based on the elbow point method (Ketchen and Shook 1996). Specifically, we tried other cluster number settings (from 2 to 20, with a step of 2) and found that a cluster number of 8 was located approximately at the elbow point. This estimated cluster number was also equal to the number of detected modules and biologically meaningful components using the traditional low-order network detection methods (see Section 2.7). During clustering, Pearson's correlation was used as similarity measurement between the prolonged feature vectors. To reduce variability in the clustering result, clustering was conducted for 50 times, each time with the initial cluster centroids positioned according to the outputs from a preliminary clustering result using randomly selected 10% subsamples. The maximum number of iterations for clustering was set to be a high value of 1×10^6, and the convergence criterion was set to be a more stringent value of 1×10^{-8} to ensure the clustering performance. The best result (i.e., the solution with the minimum within-cluster sum of point-to-centroid distances) was chosen as the final result. From the result, a cluster encompassing the cerebellum was discarded from further analysis (thus seven clusters were remained for IN-HOFC analysis, see the reason in Section 3.1) as not all subjects had cerebellum coverage during image acquisition.

Individual-Level IN-HOFC Calculation

As the originally Craddock's 200 parcellations did not arrange brain regions in a specific order, the individual FC matrix before re-arranging is somewhat jumbled (Fig. 1c). After rearranging, individual FC matrix shows a significant structured pattern with functional relevance (Fig. 1h). IN-HOFC calculation resulted in a 7×7 symmetric matrix for each subject. For visual comparison, within-group averaged IN-HOFC was generated for MCIs and CONs, respectively. A topographic representation of IN-HOFC graph with seven nodes was drawn for each group based on its averaged IN-HOFC value for easier interpretation and better visualization. Specifically, in each graph, we drew links between any pair of nodes if the absolute IN-HOFC value was larger than 0.35. This threshold was selected to ensure a fully connected graph.

Statistical Analyses

Group comparison was conducted by applying a two-sample *t*-test on each IN-HOFC link with a general linear model, consisting of the covariates of age, gender, and education level. This ensured unbiased group comparison while controlling variables of no interest. Specifically, in the full model, the dependent variable is the IN-HOFC strength of each link, out of 21 ($21 = 0.5 \times 7 \times 6$) possible links, which was further transformed into *z* score by Fisher's *r*-to-*z* transformation; independent variables were "group" (−1 for CONs and 1 for MCIs), as well as the centralized age, gender and education level. In the reduced model, the "group" variable was removed. Both full and reduced models were fitted using an ordinary least square method. The reduced sum of square of the residuals for the full model, compared with the reduced model, was used to calculate *f* and *t* statistics. Such a method is coded in both REST (http://restfmri.net/forum/REST) and SPM (http://www.fil.ion.ucl.ac.uk/spm/).

To find out whether the IN-HOFC can sensitively reflect behavior and cognitive impairment in MCIs, we conducted linear relationship between the IN-HOFC values (transformed into *z*-score by using Fisher's *r*-to-*z* transformation) and the scores from the neuropsychological assessment including MMSE and IADL, as well as those from cognitive tests including episodic memory (RI-48 cued recall), executive function (phonetic verbal fluency and trail making) and working memory (backward digital span and backward visual memory span tests). These were accomplished using the general linear model as described above. During the regression, the effects of age, gender, and education level were regarded as covariates and regressed out.

Comparison with Other Network-Wise FC Methods

It is essential to evaluate the performance of our IN-HOFC method by comparing the results with those generated based on traditional methods utilizing low-level features (i.e., BOLD time series). We first compared the functional networks generated using different methods; then we compared the sensitivity in group difference detection among all the methods. For comparison purpose, we used two mostly adopted network-wise connectivity analysis methods, modular analysis (Newman 2006) and group ICA (Calhoun et al. 2001), to generate (low-order) brain functional networks.

Network-Wise FC Via Modular Analysis

The conventional modular analysis was based on the similarity of BOLD time series among different brain regions, i.e., maximizing intra-modular FC while minimizing inter-modular FC (Newman 2006), and can be used as a low-order network FC method to compare with. Different modules can be regarded as different brain networks. Specifically, first, the individual FC matrix was calculated and the averaged FC matrix was derived across all subjects from both groups. The averaged matrix was then binarized at the network sparsity of 5% (the threshold was determined to produce a fully connected graph (Meunier et al. 2009)), based on which, modularity detection was conducted, generating group-level modules. The number of modules were not specified but were determined by the community detection algorithm. The individual

network-wise BOLD signals were derived based on the group-level modules. Specifically, for each subject, the averaged BOLD time series were extracted from each module. The network-wise FC was thus formed by cross-correlation of the module-specific BOLD time series. Group comparison on the network-wise FC was conducted between MCI group and CON group with the same method as used for IN-HOFC.

Network-Wise FC Via Group ICA

Group ICA produces brain networks based on BOLD signals (Beckmann et al. 2005) and can be further used to calculate low-order network-wise FC, or functional network connectivity (Jafri et al. 2008). GIFT version 2.0e (http://mialab.mrn.org/software/gift/) was used to generate group-level brain networks using all subjects from both groups (Calhoun et al. 2001; Zhang et al. 2010). Briefly, the fMRI data of all subjects from both MCI and CON groups were temporally concatenated, and ICA was applied to the aggregated data to ensure the decomposition results were comparable across subjects and groups. The total number of components was set to be 20 to generate large-scale functional networks (Kiviniemi et al. 2009). We used a straightforward method adapted from the previous method (Filippini et al. 2009) to calculate inter-network FC based on the ICA results. Specifically, we first identified the components of interest from the 20 components. Then, we converted the group-level t maps of the components of interest to binary masks with $p < 0.000001$, corrected by *AlphaSim*. Mean BOLD time series of each network mask were extracted from each subject's fMRI data. The pairwise correlations on the network-wise BOLD time series were calculated to generate inter-network FC result. Finally, group comparison was conducted using the same method as described above. We also did the same "functional network connectivity" analysis that directly used ICA-derived associated time series like Jafri et al. (2008).

Results

High-Order Brain Functional Networks Derived from IN-HOFC

From the clustering result, we found that all the eight clusters corresponded to meaningful brain networks (Fig. 2a). Specifically, **Cluster 1** contains 26 regions which are mainly located at the superior temporal cortices (thus we named it as the superior temporal network or ST); it also covered part of the insular, inferior frontal opercularis and putamen. It is mainly related to auditory and language functions. **Cluster 2** consists of 39 visual processing-related regions (thus was named as VIS), including the fusiform, lingual, inferior/middle/superior occipital gyrus, cuneus, calcarine and the posterior part of hippocampus/parahippocampus. **Cluster 3** compasses 27 regions including the dorsal medial and dorsal lateral frontal areas (we called it as dorsal frontal network or DF). It may be related to high-level cognitive functions such as executive control. **Cluster 4** (19 regions) is mainly in the anterior part of the inferior temporal areas (IT), including the middle/inferior temporal cortex, temporal pole, the anterior part of the hippocampus/parahippocampus, and amygdala. The main function of this high-order network is probably episodic memory. **Cluster 5** (31 regions) may be related to sensorimotor functions (SM), including the pre/postcentral gyrus, supplementary motor area, middle cingulate cortex, visuomotor area, and premotor cortex. **Cluster 6** (21 regions) locates at the ventral frontal areas (VF), including the ventral part of the anterior cingulate cortex, orbitofrontal area, caudate, olfactory cortex, rectus and part of the superior medial prefrontal cortex as well as the thalamus. This network may carry various social and emotional functions. **Cluster 7** (13 regions) contains the posterior part of the DMN, i.e., the posterior cingulate cortex, precuneus, angular gyrus, the posterior part of middle and inferior temporal gyrus, and inferior parietal lobules. *Cluster 8* exclusively covers cerebellum; however, as several of the subjects had the fMRI data which did not cover the whole cerebellum due to limited imaging field of view, this cluster was discarded from following the IN-HOFC analysis. We have spotted interesting differences between the high-order functional networks and the low-order networks in terms of spatial pattern (Section 3.5).

IN-HOFC at the Group Level

Figure 2b–c shows the group-averaged IN-HOFC matrices (weighted adjacency matrices) of MCI and CON groups, respectively. Fig. 2d–e represents the graph representation of the IN-HOFC for the two groups, with only strong (IN-HOFC >0.35) IN-HOFC shown as edges (or links, red for positive connectivity and blue for negative) connecting the nodes (i.e., high-order networks). The strength of IN-HOFC was indicated by the thickness of the edge (thin for moderate (between 0.35 and 0.5), and thick for strong (larger than 0.5) connections). The group differences can be visually identified from these group-averaged IN-HOFC matrices and graphs. Generally, the MCIs tend to have weaker IN-HOFC, especially for those between VIS and ST, and between VF and IT, as shown by the disconnections in the group-specific IN-HOFC graphs.

Statistical Group Differences in IN-HOFC

As shown in Fig. 3, there were two IN-HOFC links with statistically significant group differences ($p = 0.031$ for IN-HOFC between VIS and IT and $p = 0.034$ between VIS and ST). Specifically, the negative HOFC between VIS and IT

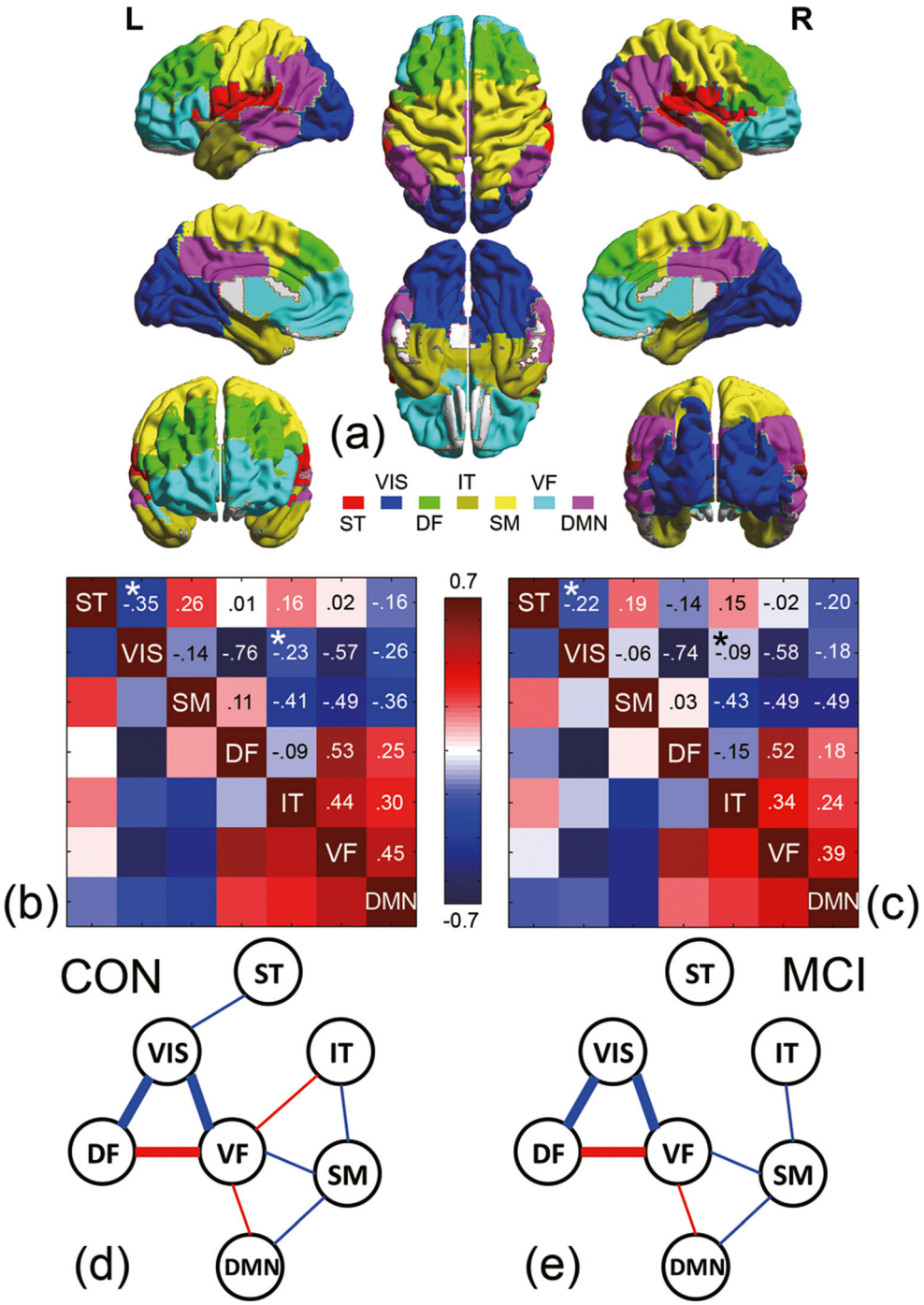

Fig. 2 Inter-Network High-Order Functional Connectivity (IN-HOFC). By *k*-means clustering on the subject-concatenated functional connectivity matrix from all subjects of both groups, high-order function networks were derived, with 7 of them shown in **(a)**. There was a network encompassing cerebellum and was discarded. The remaining 7 networks were color-coded on a brain surface for better visualization, by using BrainNet Viewer (https://www.nitrc.org/projects/bnv/). For the detailed explanation of the name abbreviation of each network, please refer to the main text. The color-coded group-averaged IN-HOFC matrices for the CON group **(b)** and MCI group **(c)** are shown with mean IN-HOFC strength. The connectivity with a significant group difference ($p < 0.05$, uncorrected) was shown with asterisks. Two graphs in **(d)** and **(e)** were the topographic representations of the IN-HOFC for CON group and MCI group, respectively. The links with the absolute averaged IN-HOFC between 0.35 and 0.5 are shown with thin lines, and those above 0.5 are shown with thick lines. Positive IN-HOFC was shown in red, and negative ones in blue

(Fig. 3a) and that between VIS and ST (Fig. 3b) in the MCIs were weaker (i.e., closer to zero), compared with those for CONs. The effect size of the group differences, measured in Cohen's *d*, was 0.35 between VIS and IT, and 0.32 between VIS and ST, which were considered to be medium. Of note, the network VIS had both reduced connectivity with the networks ST and IT, which is less likely to happen by chance, as emphasized in graph cluster-based correction methods (Han et al. 2013; Ing and Schwarzbauer 2014; Zalesky et al. 2010).

Correlation with Behavioral/Cognitive Scores

There was no significant correlation between the IN-HOFC and the behavior/cognitive scores in MCI subjects after correction for multiple comparisons.

Inter-Network Low-Order FC via Modular Analysis

The traditional low-order networks generated by module detection were shown in Fig. 4a. Seven low-order networks

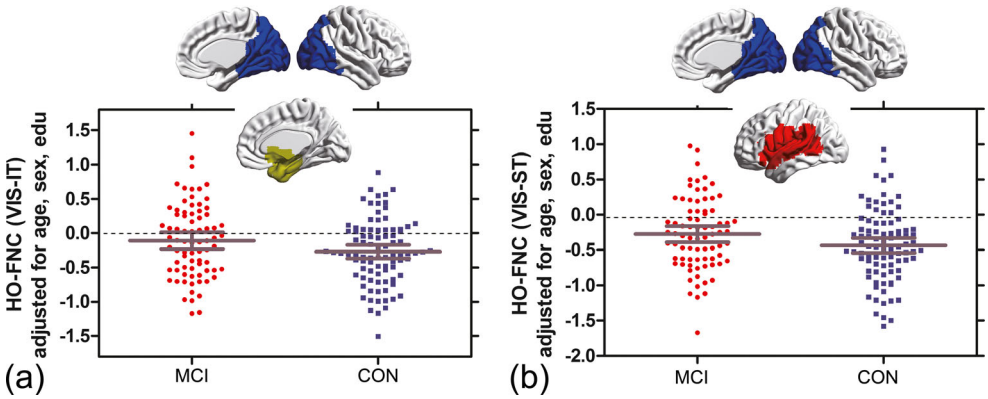

Fig. 3 Reductions of IN-HOFC for MCIs compared with CONs. The threshold was set to be $p < 0.05$ (uncorrected). The comparison was adjusted for age, gender and education level. The error bar corresponds to a 95% confidence interval, and the middle line corresponds to the mean IN-HOFC strength

except the cerebellar network were visually compared with the high-order networks produced by our method. The spatial patterns of the modules for VIS, DMN and IT are roughly similar to the corresponding high-order networks derived by our method, except that the low-order DMN did not include posterior temporal lobe and the low-order IT extended to cover more temporal and orbitofrontal cortices. The other low-order networks, DF, SM, and ST, changed a lot compared with our high-order networks. Specifically, the low-order DF includes large areas that belonged to the high-order VF; and the basal ganglia (BG) and thalamus were singled out as a new low-order network (there was no low-order VF). The spatial distribution of the low-order ST was increased, occupying more lateral temporal areas and the areas previously belonging to the high-order SM. In summary, the high-order brain networks show interestingly different spatial patterns compared to the traditional low-order brain networks.

Group comparison with FC among these modules revealed that only the low-order inter-network FC between the VIS and ST was significantly ($p = 0.037$) reduced in MCIs compared to the CONs. All other inter-network low-order FC had no significant group difference ($p > 0.05$).

Inter-Network Low-Order FC Via Group ICA

We identified eight components based on their spatial similarity to the previously reported functional networks (Beckmann et al. 2005; Varoquaux and Craddock 2013). The component covering cerebellum was discarded due to the same reason. All the remained seven networks are shown in Fig. 4b with similar color-coding to that used for high-order networks; together they cover the most part of the brain. Specifically, the components VIS, DF, VF, and DMN were quite similar to the corresponding high-order networks. The component SM covered smaller areas compared with high-order SM. There were two components covering the whole temporal lobe: T1 and T2. The component T1 encompasses most of the superior temporal cortex and ventral central regions (most of these regions belonged to a high-order network SM); the component T2 included the entire middle temporal cortex as well as a part of the superior and inferior cortices. The major difference between the low-order networks T1/T2 and the high-order networks ST/IT was that no medial part of the temporal region was included. Based on the mean BOLD signals extracted from the 7 components, inter-network FC analysis found no significant group difference ($p > 0.05$). If using ICA-derived component-associated time courses, inter-network FC analysis found a group difference between the components of DMN and T1 (mostly covering the superior temporal cortex) ($p = 0.019$, $t = -2.37$), where the MCI group had increased negative connectivity compared with the CONs. No other group difference was found.

Discussion

General Discussion

In this paper, we proposed an inter-network high-order functional connectivity (IN-HOFC) analysis method and demonstrated its effectiveness in the detection of potential AD biomarkers. The new method is a network-level extension of a region-level HOFC that was originally proposed to measure the pair-wise similarity of FC topographic profiles, reflecting high-level brain functional relationship, between two brain regions (Zhang et al. 2016a). Compared to the traditional, low-order, BOLD signal synchronization-based FC, HOFC can result in improved sensitivity for group difference detection (Zhang et al. 2016a) and can provide supplementary information to the low-order FC (Jia et al. 2017; Zhang et al. 2016a). To further investigate high-order functional hierarchy, i.e., the high-order functional relationship between large-scale networks, it is necessary to extend the region-wise HOFC to network-wise HOFC, where the FC topographic profiles can further be used to generate a different set of functional networks and the similarity between network-wise FC topographic profiles can be assessed. The IN-HOFC method was shown to be able to capture more information than the

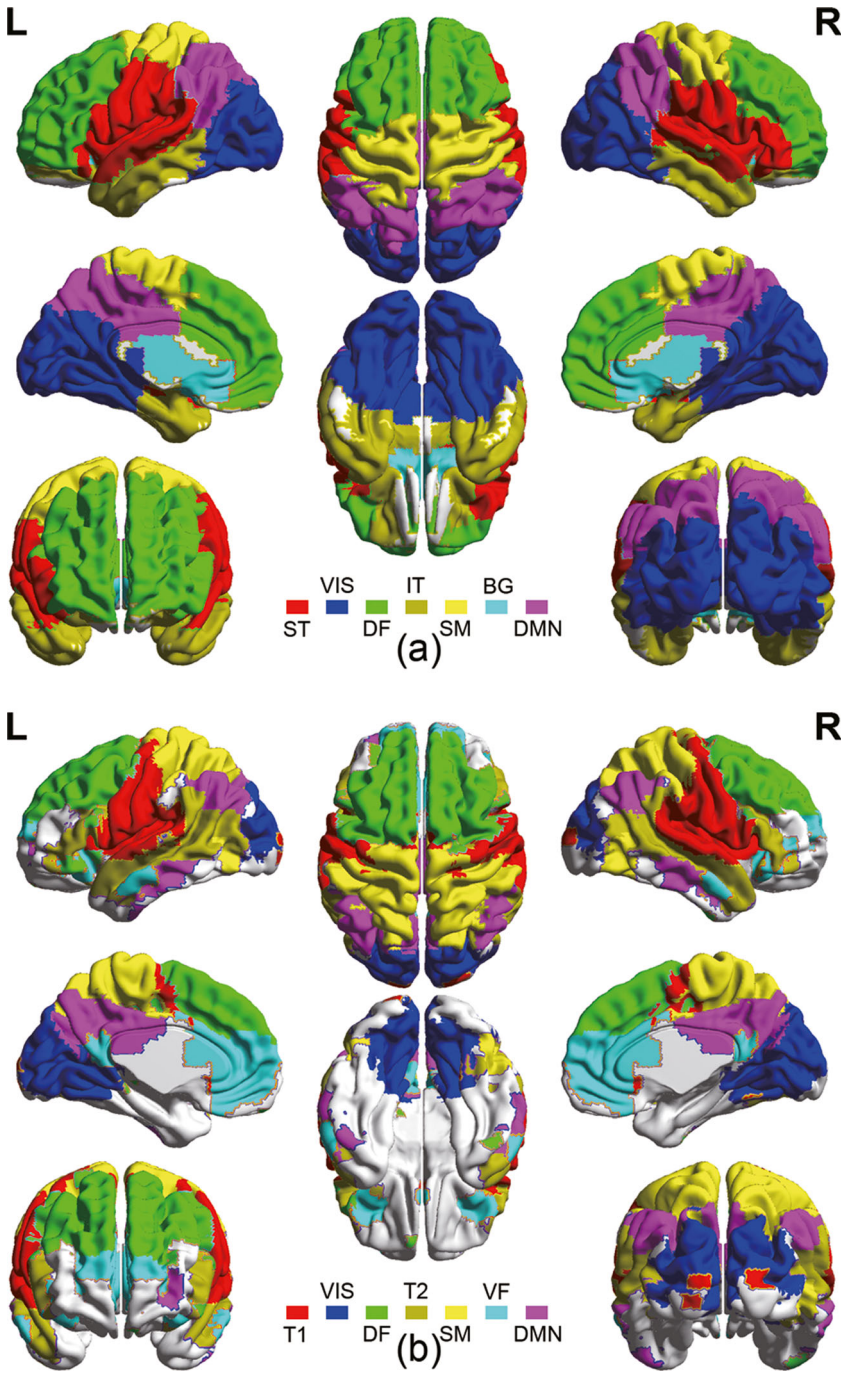

Fig. 4 Networks generated by using low-level features. The group-level networks generated by modular analysis, based on BOLD time series (low-level features), were shown in Panel **(a)**. The group-level networks (*t*-maps with a threshold of $p < 0.000001$) derived from group ICA, based on BOLD fMRI data, were shown in Panel **(b)**. All the networks were color-coded on a brain surface for better visualization, by using BrainNet Viewer (https://www.nitrc.org/projects/bnv/). For the detailed explanation of the name abbreviation of each network, please refer to the main text

traditional functional network connectivity methods, which may be important to better distinguish the diseased cohorts from the healthy controls. The IN-HOFC was applied to compare between MCI and normal elderly subjects, showing improved sensitivity in group difference detection (Figs. 2 and 3). Reduction of the IN-HOFC for two pairs of high-order functional networks, i.e., VIS–IT and VIS–ST, were found to be potential biomarkers of MCI (Fig. 3). Our method can be easily applied to other disease studies in the future, as a necessary supplement to traditional network FC analysis.

Better Performance of IN-HOFC in Biomarker Detection

The low-level feature (BOLD signals) based inter-network FC analysis, as represented by modular analysis and ICA, revealed different spatial configurations of the brain networks (Fig. 4) compared to the high-order networks (Fig. 2a). The differences are more prominent for the high-level cognition-related networks located in the temporal and frontal lobes. For example, the IT network was not found by ICA and is also

found more laterally distributed according to the results from the modular analysis. Such a different spatial pattern may cause the performance difference between inter-network FC and IN-HOFC. Specifically, the modular analysis only found VIS–ST had group difference, but nothing was found for the IT network. Using group ICA-derived inter-network FC, still, no group difference was found. By directly using the time series associated with the components to calculate inter-network FC, we found a group difference between the posterior DMN and the superior temporal network. There is no group difference found for other higher cognition related inter-network FC. The reasons are two folds.

The first reason for IN-HOFC's superior performance than other low-order inter-network FC methods roots from the unique characteristic of HOFC. FC topological profile of a brain region carries information about how other regions functionally connected with it, like a "fingerprint" to this brain region. With a similar fingerprint, we assume that the two regions are quite close in the FC space. However, such a topological closeness may not hold in the BOLD signal space or equal to BOLD synchronization-based relationship. Another reason is that IN-HOFC is based on correlation (FC features)'s correlation, which makes it less sensitive to the global noise. Such type of noise is common, mainly contributed by the physiological fluctuations and difficult to remove thoroughly from the rs-fMRI signals. Such noise can globally increase or decrease internetwork FC but could minimally affect IN-HOFC, because the second round of correlation analysis can largely remove such global noise in the FCs. In the future, more datasets should be used to further validate the increment of the sensitivity using IN-HOFC.

Innovation and Biological Meaning of IN-HOFC

It is not trivial to understand the biological meaning of the high-order functional networks revealed by our method. The unique spatial patterns of the high-order networks derived by FC topographical profiles could be indicative. First, the SM-related high-order network is prominently enlarged compared to the low-order FC-based networks, with many high-level motor-related regions in the association areas included. Second, the frontal lobe was separated into two (ventral and dorsal) high-order subnetworks. Third, the temporal lobe was further separated into three (anterior-inferior, superior, and posterior) high-order subnetworks. All of these differences indicate a fundamental difference between the high-order and traditional low-order networks, with the latter more constrained by the spatial proximity. That is, the low-order functional networks are more likely to be confined to their respective lobes, while the high-order networks reflect a larger functional-anatomical discrepancy, possibly due to more functional segregation in terms of high-level functions. Finally, the thalamus was connected with the ventral medial and ventral lateral frontal areas, showing their much closer relationship in a high-order manner.

We highlighted two innovations in our IN-HOFC method. First, the brain functional network definition is high order, because the inputs to the clustering analysis are FC topographic profiles of all brain regions, which contains high-level information. The brain regions with highly similar FC topographic profiles are grouped together. A group-level *k*-means clustering scheme was adopted to produce high-order networks while preserving network correspondence across subjects, making group comparison feasible. Second, in network-level FC analysis, network-specific FC topographic profiles were used for the second round of connectivity analysis, which further reveals the functional hierarchy of the HOFC. In summary, we addressed the two critical issues (i.e., network *definition* and *connectivity*) from a high-order functional relationship point of view.

The biological meaning of the IN-HOFC might be interpreted as an indirect connectivity between two functional systems. To understand IN-HOFC, firstly one needs to understand how high-order functional networks were generated. In our method, the functional relevance between any pair of brain regions is assessed by the similarity between their FC topographic profiles. If two regions are similarity connected with other regions, they are inherently mutually connected because both of them could be similarly modulated or mediated by the same group of other regions. In this perspective, we can define whether two regions are connected in a high-order manner and group them into the same high-order functional network. The concept is similar to that used for functional parcellation (Cohen et al. 2008; Hirose et al. 2013; Nelson et al. 2010), in mass-univariate analysis between behavioral measurement and subject-wise FC profiles (Smith et al. 2013), and in across-subject spatial covariance-based connectivity (He et al. 2008). From the feature space point of view, traditional pairwise FC measures the distance between two regions in a low-order feature space with the dimensionality equal to the number of BOLD time points; in contrast, HOFC measures the distance in another space spanned by higher-level FC features. Future studies should be conducted to further understand the biological meaning of IN-HOFC using manipulated connections as gold standard using animal models.

The IN-HOFC does not necessarily equal or proportional to traditional internetwork FC. To better understand this, we can think of a much simpler case, i.e., the difference between the regional-wise HOFC and traditional low-order FC. As we have demonstrated in our previous paper (Zhang et al. 2016a), in general, HOFC magnifies FC in a nonlinear way. By strengthening the backbone connectivities, HOFC may strength the group difference. For several connections, weak FC corresponds to strong HOFC because of the two regions have more similar FC topography than BOLD time courses.

For example, it is shown that dorsal anterior cingulate cortex is well connected to the posterior cingulate cortex in terms of HOFC, although they are not generally believed in the same functional network, with a low FC (Zhang et al. 2016a). The difference between HOFC and FC can also be proved based on the fact that using HOFC features can boost the performance of individualized classification compared to FC features. In a consciousness level prediction study using acquired brain traumatic injury patients, HOFC was shown to have increased the classification accuracy by more than 10% compared to FC (Jia et al. 2017). Of note, we by no means advocate that IN-HOFC is anatomically real connections among networks, but is actually an indirect connectivity, contributed by the similarity on the overall common topographical property between all within-network regions from one network and those from another network.

Studies on the relationship between different brain functional networks have relatively a short history. Previously, group comparison on a single network was dominant in the field, mainly focusing on the DMN (Greicius et al. 2004). By Seeley et al. (2007), the relationship between salience and executive control networks was investigated. Jafri et al. (2008) first investigated functional network connectivity among ICA-derived networks. ICA-based inter-network FC has been intensively used in both basic and clinical neuroscience studies (Karunanayaka et al. 2014; Kong et al. 2014; Menon 2011; Wang et al. 2014). These studies were based on a hypothesis that spatially independent components may have a temporal relationship as revealed by similar BOLD activities or co-activity. Similarly, based on similar temporal activity pattern, Newman (2006) established a modularity detection algorithm for complex network analysis. A module has commonly been interpreted as a functional network, and inter-modular connectivity can be calculated to represent inter-network FC. While the network definition and hypotheses are different for these two types of methods, they both use BOLD signals for calculation of FC. Our IN-HOFC provides a feasible and simple way for future studies to investigate the high-order, more complex functional relationship between the large-scale functional networks.

Potential Implications of MCI Detection

As a result, our method found an important high-order network, IT, in the middle/inferior temporal cortex, temporal pole, the head of hippocampus/parahippocampus, and amygdala. The probable function mediated by this network is episodic memory (Touroutoglou et al. 2015), emotional memory (van Eijndhoven et al. 2011), semantic memory (Bonner and Price 2013; Ryan et al. 2010), autobiographical processing (Trinkler et al. 2009), and multisensory integration (Misic et al. 2014). This network is also highly involved in AD pathology, especially the regions in entorhinal cortex and piriform (Brier et al. 2012; Di Paola et al. 2007; Tromp et al. 2015). The other two methods under comparison *either* failed in the detection of such network (Fig. 4b) *or* failed in separation from other networks (Fig. 4a). This may result in no group difference found in FC with the IT network from both modular analysis and ICA methods. Many previous studies, focusing on only conventional FC among functional networks, constructed networks based on correlation of BOLD time series. For example, Brier et al. (2012) used a seed-based correlation to identify five networks but none of them resembles our high-order IT network. Their finding is that AD progression is related to a gradual disturbance between the DMN and the dorsal attention network as well as the SM. On the other side, some famous ICA papers (Varoquaux et al. 2010) suggested that the anterior temporal network is not biologically meaningful while others believed this network was related to memory function (Gour et al. 2011). Our result suggested that this network is biologically meaningful and the functional connectivity with this network could be a putative biomarker for MCI identification.

Another interesting finding is that we found a high-order functional relationship among specific sub-divisions in the temporal lobe might be sensitive to MCI identification. IN-HOFC analysis revealed that three networks, i.e., ST, IT and VIS (Fig. 2a), encompassed the temporal lobe. Spatially, IT covered the anterior, inferior and medial parts of the temporal lobe (including the entorhinal cortex), VIS included the posterior and medial parts and ST located mainly in the superior part of the temporal lobe. The reduced high-order interaction among them (Fig. 3) can be summarized as the disconnection of inter-network connectivity between the anterior and posterior portions of the medial temporal lobe (VIS–IT), and also between the lateral and medial temporal areas (VIS–ST). Interestingly, a previous study using different data sets, different imaging modality (diffusion tensor imaging) and different connectivity metric (structural connectivity) also suggested that inter-network interaction, rather than within-network connectivity, between cognition and perception domain, is valuable for distinguishing MCI and normal controls (Zhu et al. 2014). These "triple subnetworks" are suggested to be potential reliable biomarkers for MCI detection.

Limitations

In this study, regionally averaged BOLD signals were first calculated to obtain FC topographic profiles. Such an FC fingerprint depends on the initial parcellation of the brain. Different parcellation atlases may result in different FC profiles and could affect the clustering and following IN-HOFC results. There have been several popular atlases provided by previous studies (Desikan et al. 2006; Dosenbach et al. 2010). In the future, different initial brain parcellation methods should be used and the potential effect to the final IN-HOFC

results should be evaluated (Eickhoff et al. 2015). There is another issue in the group-level clustering framework. In the current study, we followed a two-step analysis strategy by first conducting a group-level analysis on the concatenated individual data and then performing individual-level analysis based on the group templates. This is a common computational strategy for data-driven analysis (Zhang et al. 2010), which balances well between sensitive individual variability detection and maintaining component correspondence across subjects. The drawback is the potential reduced effect size in a group comparison due to pooling all subjects from both groups together to calculate group-level clusters. Another concern regarding the two-layer of correlation analyses in IN-HOFC calculation is that there could be accumulated statistical error caused by this hierarchical style of correlations. Finally, in the experiment, we conducted the MCI diagnosis purely using clinical scores. Several studies have shown promising MCI diagnosis using new neurobiological features (Frisoni and Coleman 2011). We speculate that a more accurate and objective diagnosis method may further improve our result.

Conclusions

Our proposed inter-network high-order functional connectivity (IN-HOFC) method extends our previous regional pairwise HOFC method to a higher-level network interaction analysis. Biologically meaningful and clinically discriminative high-order functional networks and also their high-order functional relationship was demonstrated with group comparison between MCIs and normal controls. IN-HOFC was also proved to be sensitive in capturing subtle abnormality in high-order network interaction in MCIs, which could be the promising biomarkers for early AD diagnosis.

Information Sharing Statement

The code for inter-network high-order functional connectivity analysis will be shared upon individual inquiry to the corresponding author, Dr. Dinggang Shen or Dr. Han Zhang (hanzhang@med.unc.edu). According to the data protection policy of the collaborating institution, direct general public access is not available. However, individual researchers are suggested to contact Dr. Sven Haller (sven.haller@gmail.com) for more information about the data used in this study.

Acknowledgments This work is supported in part by NIH grants (EB006733, EB008374, EB009634, MH100217, AG041721, AG049371 and AG042599). We have no conflict of interest to declare.

References

Allen, E. A., Erhardt, E. B., Damaraju, E., Gruner, W., Segall, J. M., Silva, R. F., Havlicek, M., Rachakonda, S., Fries, J., Kalyanam, R., Michael, A. M., Caprihan, A., Turner, J. A., Eichele, T., Adelsheim, S., Bryan, A. D., Bustillo, J., Clark, V. P., Feldstein Ewing, S. W., Filbey, F., Ford, C. C., Hutchison, K., Jung, R. E., Kiehl, K. A., Kodituwakku, P., Komesu, Y. M., Mayer, A. R., Pearlson, G. D., Phillips, J. P., Sadek, J. R., Stevens, M., Teuscher, U., Thoma, R. J., & Calhoun, V. D. (2011). A baseline for the multivariate comparison of resting-state networks. *Front Syst Neurosci, 5*, 2.

Bai, F., Zhang, Z., Yu, H., Shi, Y., Yuan, Y., Zhu, W., Zhang, X., & Qian, Y. (2008). Default-mode network activity distinguishes amnestic type mild cognitive impairment from healthy aging: A combined structural and resting-state functional MRI study. *Neurosci Lett, 438*, 111–115.

Barkhof, F., Haller, S., & Rombouts, S. A. (2014). Resting-state functional MR imaging: A new window to the brain. *Radiology, 272*, 29–49.

Beckmann, C. F., DeLuca, M., Devlin, J. T., & Smith, S. M. (2005). Investigations into resting-state connectivity using independent component analysis. *Philos Trans R Soc Lond Ser B Biol Sci, 360*, 1001–1013.

Bellec, P., Rosa-Neto, P., Lyttelton, O. C., Benali, H., & Evans, A. C. (2010). Multi-level bootstrap analysis of stable clusters in resting-state fMRI. *Neuroimage, 51*, 1126–1139.

Bijsterbosch, J., Smith, S., Forster, S., John, O. P., & Bishop, S. J. (2014). Resting state correlates of subdimensions of anxious affect. *J Cogn Neurosci, 26*, 914–926.

Bonner, M. F., & Price, A. R. (2013). Where is the anterior temporal lobe and what does it do? *J Neurosci, 33*, 4213–4215.

Brier, M. R., Thomas, J. B., Snyder, A. Z., Benzinger, T. L., Zhang, D., Raichle, M. E., Holtzman, D. M., Morris, J. C., & Ances, B. M. (2012). Loss of intranetwork and internetwork resting state functional connections with Alzheimer's disease progression. *J Neurosci, 32*, 8890–8899.

Bullmore, E., & Sporns, O. (2009). Complex brain networks: Graph theoretical analysis of structural and functional systems. *Nat Rev Neurosci, 10*, 186–198.

Calhoun, V. D., Adali, T., Pearlson, G. D., & Pekar, J. J. (2001). A method for making group inferences from functional MRI data using independent component analysis. *Hum Brain Mapp, 14*, 140–151.

Cohen, A. L., Fair, D. A., Dosenbach, N. U., Miezin, F. M., Dierker, D., Van Essen, D. C., Schlaggar, B. L., & Petersen, S. E. (2008). Defining functional areas in individual human brains using resting functional connectivity MRI. *Neuroimage, 41*, 45–57.

Cordes, D., Haughton, V., Carew, J. D., Arfanakis, K., & Maravilla, K. (2002). Hierarchical clustering to measure connectivity in fMRI resting-state data. *Magn Reson Imaging, 20*, 305–317.

Craddock, R. C., James, G. A., Holtzheimer, P. E., 3rd, Hu, X. P., & Mayberg, H. S. (2012). A whole brain fMRI atlas generated via spatially constrained spectral clustering. *Hum Brain Mapp, 33*, 1914–1928.

Desikan, R. S., Segonne, F., Fischl, B., Quinn, B. T., Dickerson, B. C., Blacker, D., Buckner, R. L., Dale, A. M., Maguire, R. P., Hyman, B. T., Albert, M. S., & Killiany, R. J. (2006). An automated labeling system for subdividing the human cerebral cortex on MRI scans into gyral based regions of interest. *Neuroimage, 31*, 968–980.

Di Paola, M., Macaluso, E., Carlesimo, G. A., Tomaiuolo, F., Worsley, K. J., Fadda, L., & Caltagirone, C. (2007). Episodic memory impairment in patients with Alzheimer's disease is correlated with

entorhinal cortex atrophy. A voxel-based morphometry study. *Journal of Neurology, 254*, 774–781.

Dosenbach, N. U., Nardos, B., Cohen, A. L., Fair, D. A., Power, J. D., Church, J. A., Nelson, S. M., Wig, G. S., Vogel, A. C., Lessov-Schlaggar, C. N., Barnes, K. A., Dubis, J. W., Feczko, E., Coalson, R. S., Pruett, J. R., Jr., Barch, D. M., Petersen, S. E., & Schlaggar, B. L. (2010). Prediction of individual brain maturity using fMRI. *Science, 329*, 1358–1361.

Eickhoff, S. B., Thirion, B., Varoquaux, G., & Bzdok, D. (2015). Connectivity-based parcellation: Critique and implications. *Hum Brain Mapp, 36*, 4771–4792.

Filippini, N., MacIntosh, B. J., Hough, M. G., Goodwin, G. M., Frisoni, G. B., Smith, S. M., Matthews, P. M., Beckmann, C. F., & Mackay, C. E. (2009). Distinct patterns of brain activity in young carriers of the APOE-epsilon4 allele. *Proc Natl Acad Sci U S A, 106*, 7209–7214.

Frisoni, G. B., & Coleman, P. D. (2011). Mild cognitive impairment: Instructions for use at neurobiology of aging. Neurobiology of aging. *Neurobiology of Aging, 32*, 761–762.

Gour, N., Ranjeva, J. P., Ceccaldi, M., Confort-Gouny, S., Barbeau, E., Soulier, E., Guye, M., Didic, M., & Felician, O. (2011). Basal functional connectivity within the anterior temporal network is associated with performance on declarative memory tasks. *Neuroimage, 58*, 687–697.

Greicius, M. (2008). Resting-state functional connectivity in neuropsychiatric disorders. *Curr Opin Neurol, 21*, 424–430.

Greicius, M. D., Srivastava, G., Reiss, A. L., & Menon, V. (2004). Default-mode network activity distinguishes Alzheimer's disease from healthy aging: Evidence from functional MRI. *Proc Natl Acad Sci U S A, 101*, 4637–4642.

Han, C. E., Yoo, S. W., Seo, S. W., Na, D. L., & Seong, J. K. (2013). Cluster-based statistics for brain connectivity in correlation with behavioral measures. *PLoS One, 8*, e72332.

He, Y., Chen, Z., & Evans, A. (2008). Structural insights into aberrant topological patterns of large-scale cortical networks in Alzheimer's disease. *J Neurosci, 28*, 4756–4766.

Hirose, S., Watanabe, T., Wada, H., Imai, Y., Machida, T., Shirouzu, I., Miyashita, Y., & Konishi, S. (2013). Functional relevance of micromodules in the human association cortex delineated with high-resolution FMRI. *Cereb Cortex, 23*, 2863–2871.

Ing, A., & Schwarzbauer, C. (2014). Cluster size statistic and cluster mass statistic: Two novel methods for identifying changes in functional connectivity between groups or conditions. *PLoS One, 9*, e98697.

Jafri, M. J., Pearlson, G. D., Stevens, M., & Calhoun, V. D. (2008). A method for functional network connectivity among spatially independent resting-state components in schizophrenia. *Neuroimage, 39*, 1666–1681.

Jia, X., Zhang, H., Adeli, E., & Shen, D. (2017). 2017. Consciousness level and recovery outcome prediction using high-order brain functional connectivity network. *Connectomics Neuroimaging, 10511*, 17–24.

Karunanayaka, P., Eslinger, P. J., Wang, J. L., Weitekamp, C. W., Molitoris, S., Gates, K. M., Molenaar, P. C., & Yang, Q. X. (2014). Networks involved in olfaction and their dynamics using independent component analysis and unified structural equation modeling. *Hum Brain Mapp, 35*, 2055–2072.

Ketchen, D. J., & Shook, C. L. (1996). The application of cluster analysis in strategic management research: An analysis and critique. *Strateg Manag J, 17*, 441–458.

Kiviniemi, V., Starck, T., Remes, J., Long, X., Nikkinen, J., Haapea, M., Veijola, J., Moilanen, I., Isohanni, M., Zang, Y. F., & Tervonen, O. (2009). Functional segmentation of the brain cortex using high model order group PICA. *Hum Brain Mapp, 30*, 3865–3886.

Kong, Y., Eippert, F., Beckmann, C. F., Andersson, J., Finsterbusch, J., Buchel, C., Tracey, I., & Brooks, J. C. (2014). Intrinsically organized resting state networks in the human spinal cord. *Proc Natl Acad Sci U S A, 111*, 18067–18072.

Lee, M. H., Hacker, C. D., Snyder, A. Z., Corbetta, M., Zhang, D., Leuthardt, E. C., & Shimony, J. S. (2012). Clustering of resting state networks. *PLoS One, 7*, e40370.

Li, H. J., Hou, X. H., Liu, H. H., Yue, C. L., He, Y., & Zuo, X. N. (2015). Toward systems neuroscience in mild cognitive impairment and Alzheimer's disease: A meta-analysis of 75 fMRI studies. *Hum Brain Mapp, 36*, 1217–1232.

Liang, P., Zhang, H., Xu, Y., Jia, W., Zang, Y., & Li, K. (2015). Disruption of cortical integration during midazolam-induced light sedation. *Hum Brain Mapp, 36*, 4247–4261.

Menon, V. (2011). Large-scale brain networks and psychopathology: A unifying triple network model. *Trends Cogn Sci, 15*, 483–506.

Meunier, D., Achard, S., Morcom, A., & Bullmore, E. (2009). Age-related changes in modular organization of human brain functional networks. *Neuroimage, 44*, 715–723.

Mezer, A., Yovel, Y., Pasternak, O., Gorfine, T., & Assaf, Y. (2009). Cluster analysis of resting-state fMRI time series. *Neuroimage, 45*, 1117–1125.

Misic, B., Goni, J., Betzel, R. F., Sporns, O., & McIntosh, A. R. (2014). A network convergence zone in the hippocampus. *PLoS Comput Biol, 10*, e1003982.

Misic, B., Betzel, R. F., Nematzadeh, A., Goni, J., Griffa, A., Hagmann, P., Flammini, A., Ahn, Y. Y., & Sporns, O. (2015). Cooperative and competitive spreading dynamics on the human connectome. *Neuron, 86*, 1518–1529.

Nelson, S. M., Cohen, A. L., Power, J. D., Wig, G. S., Miezin, F. M., Wheeler, M. E., Velanova, K., Donaldson, D. I., Phillips, J. S., Schlaggar, B. L., & Petersen, S. E. (2010). A parcellation scheme for human left lateral parietal cortex. *Neuron, 67*, 156–170.

Newman, M. E. (2006). Modularity and community structure in networks. *Proc Natl Acad Sci U S A, 103*, 8577–8582.

Nickl-Jockschat, T., Kleiman, A., Schulz, J. B., Schneider, F., Laird, A. R., Fox, P. T., Eickhoff, S. B., & Reetz, K. (2012). Neuroanatomic changes and their association with cognitive decline in mild cognitive impairment: A meta-analysis. *Brain Struct Funct, 217*, 115–125.

Petersen, R. C., Doody, R., Kurz, A., Mohs, R. C., Morris, J. C., Rabins, P. V., Ritchie, K., Rossor, M., Thal, L., & Winblad, B. (2001). Current concepts in mild cognitive impairment. *Arch Neurol, 58*, 1985–1992.

Putcha, D., Ross, R. S., Cronin-Golomb, A., Janes, A. C., & Stern, C. E. (2015). Altered intrinsic functional coupling between core neurocognitive networks in Parkinson's disease. *Neuroimage Clin, 7*, 449–455.

Qiao, L., Zhang, H., Kim, M., Teng, S., Zhang, L., & Shen, D. (2016). Estimating functional brain networks by incorporating a modularity prior. *Neuroimage, 141*, 399–407.

Richiardi, J., Monsch, A. U., Haas, T., Barkhof, F., Van de Ville, D., Radu, E. W., Kressig, R. W., & Haller, S. (2015). Altered cerebrovascular reactivity velocity in mild cognitive impairment and Alzheimer's disease. *Neurobiol Aging, 36*, 33–41.

Ryan, L., Lin, C. Y., Ketcham, K., & Nadel, L. (2010). The role of medial temporal lobe in retrieving spatial and nonspatial relations from episodic and semantic memory. *Hippocampus, 20*, 11–18.

Seeley, W. W., Menon, V., Schatzberg, A. F., Keller, J., Glover, G. H., Kenna, H., Reiss, A. L., & Greicius, M. D. (2007). Dissociable intrinsic connectivity networks for salience processing and executive control. *J Neurosci, 27*, 2349–2356.

Smith, S. M., Vidaurre, D., Beckmann, C. F., Glasser, M. F., Jenkinson, M., Miller, K. L., Nichols, T. E., Robinson, E. C., Salimi-Khorshidi, G., Woolrich, M. W., Barch, D. M., Ugurbil, K., & Van Essen, D. C. (2013). Functional connectomics from resting-state fMRI. *Trends Cogn Sci, 17*, 666–682.

Sporns, O., & Betzel, R. F. (2016). Modular brain networks. *Annu Rev Psychol, 67*, 613–640.

Stam, C. J., van Straaten, E. C., Van Dellen, E., Tewarie, P., Gong, G., Hillebrand, A., Meier, J., & Van Mieghem, P. (2016). The relation between structural and functional connectivity patterns in complex brain networks. *Int J Psychophysiol, 103*, 149–160.

Stevens, M. C., Pearlson, G. D., & Calhoun, V. D. (2009). Changes in the interaction of resting-state neural networks from adolescence to adulthood. *Hum Brain Mapp, 30*, 2356–2366.

Supekar, K., Menon, V., Rubin, D., Musen, M., & Greicius, M. D. (2008). Network analysis of intrinsic functional brain connectivity in Alzheimer's disease. *PLoS Comput Biol, 4*, e1000100.

Touroutoglou, A., Andreano, J. M., Barrett, L. F., & Dickerson, B. C. (2015). Brain network connectivity-behavioral relationships exhibit trait-like properties: Evidence from hippocampal connectivity and memory. *Hippocampus, 25*, 1591–1598.

Trinkler, I., King, J. A., Doeller, C. F., Rugg, M. D., & Burgess, N. (2009). Neural bases of autobiographical support for episodic recollection of faces. *Hippocampus, 19*, 718–730.

Tromp, D., Dufour, A., Lithfous, S., Pebayle, T., & Despres, O. (2015). Episodic memory in normal aging and Alzheimer disease: Insights from imaging and behavioral studies. *Ageing Res Rev, 24*, 232–262.

van Eijndhoven, P., van Wingen, G., Fernandez, G., Rijpkema, M., Verkes, R. J., Buitelaar, J., & Tendolkar, I. (2011). Amygdala responsivity related to memory of emotionally neutral stimuli constitutes a trait factor for depression. *Neuroimage, 54*, 1677–1684.

Varoquaux, G., & Craddock, R. C. (2013). Learning and comparing functional connectomes across subjects. *Neuroimage, 80*, 405–415.

Varoquaux, G., Sadaghiani, S., Pinel, P., Kleinschmidt, A., Poline, J. B., & Thirion, B. (2010). A group model for stable multi-subject ICA on fMRI datasets. *Neuroimage, 51*, 288–299.

Wang, D., Qin, W., Liu, Y., Zhang, Y., Jiang, T., & Yu, C. (2014). Altered resting-state network connectivity in congenital blind. *Hum Brain Mapp, 35*, 2573–2581.

Wang, S. F., Ritchey, M., Libby, L. A., & Ranganath, C. (2016). Functional connectivity based parcellation of the human medial temporal lobe. *Neurobiology of Learning and Memory, 134*(Pt A), 123–134.

Wig, G. S., Laumann, T. O., & Petersen, S. E. (2014). An approach for parcellating human cortical areas using resting-state correlations. *Neuroimage, 93*(Pt 2), 276–291.

Yang, S. Q., Xu, Z. P., Xiong, Y., Zhan, Y. F., Guo, L. Y., Zhang, S., Jiang, R. F., Yao, Y. H., Qin, Y. Y., Wang, J. Z., Liu, Y., & Zhu, W. Z. (2016). Altered Intranetwork and internetwork functional connectivity in type 2 diabetes mellitus with and without cognitive impairment. *Sci Rep, 6*, 32980.

Yao, Z., Zhang, Y., Lin, L., Zhou, Y., Xu, C., & Jiang, T. (2010). Abnormal cortical networks in mild cognitive impairment and Alzheimer's disease. *PLoS Comput Biol, 6*, e1001006.

Yeo, B. T., Krienen, F. M., Sepulcre, J., Sabuncu, M. R., Lashkari, D., Hollinshead, M., Roffman, J. L., Smoller, J. W., Zollei, L., Polimeni, J. R., Fischl, B., Liu, H., & Buckner, R. L. (2011). The organization of the human cerebral cortex estimated by intrinsic functional connectivity. *J Neurophysiol, 106*, 1125–1165.

Zalesky, A., Fornito, A., & Bullmore, E. T. (2010). Network-based statistic: Identifying differences in brain networks. *Neuroimage, 53*, 1197–1207.

Zhang, D., & Raichle, M. E. (2010). Disease and the brain's dark energy. *Nat Rev Neurol, 6*, 15–28.

Zhang, H., Zuo, X. N., Ma, S. Y., Zang, Y. F., Milham, M. P., & Zhu, C. Z. (2010). Subject order-independent group ICA (SOI-GICA) for functional MRI data analysis. *Neuroimage, 51*, 1414–1424.

Zhang, H., Chen, X., Shi, F., Li, G., Kim, M., Giannakopoulos, P., Haller, S., & Shen, D. (2016a). Topographical information-based high-order functional connectivity and its application in abnormality detection for mild cognitive impairment. *J Alzheimers Dis, 54*, 1095–1112.

Zhang, J., Cheng, W., Liu, Z., Zhang, K., Lei, X., Yao, Y., Becker, B., Liu, Y., Kendrick, K. M., Lu, G., & Feng, J. (2016b). Neural, electrophysiological and anatomical basis of brain-network variability and its characteristic changes in mental disorders. *Brain, 139*, 2307–2321.

Zhang, H., Chen, X., Zhang, Y., & Shen, D. (2017a). Test-retest reliability of "high-order" functional connectivity in young healthy adults. *Front Neurosci, 11*, 439.

Zhang, Y., Zhang, H., Chen, X., Lee, S. W., & Shen, D. (2017b). Hybrid high-order functional connectivity networks using resting-state functional MRI for mild cognitive impairment diagnosis. *Sci Rep, 7*, 6530.

Zhang, Y., Zhang, H., Chen, X., & Shen, D. (2017c). Constructing multi-frequency high-order functional connectivity network for diagnosis of mild cognitive impairment. *Connectomics Neuroimaging, 2017*(10511), 9–16.

Zhao, F., Zhang, H., Rekik, I., An, Z., & Shen, D. (2018). Diagnosis of autism Spectrum disorders using multi-level high-order functional networks derived from resting-state functional MRI. *Front Hum Neurosci, 12*, 184.

Zhu, D., Li, K., Terry, D. P., Puente, A. N., Wang, L., Shen, D., Miller, L. S., & Liu, T. (2014). Connectome-scale assessments of structural and functional connectivity in MCI. *Hum Brain Mapp, 35*, 2911–2923.